The Role of Baroclinic Processes in Tropical Cyclone Motion: The Influence of Vertical Tilt

MARIA FLATAU

Scripps Institution of Oceanography, University of California San Diego, La Jolla, California

WAYNE H. SCHUBERT

Department of Atmospheric Science, Colorado State University, Fort Collins, Colorado

DUANE E. STEVENS

Department of Meteorology, University of Hawaii, Honolulu, Hawaii

(Manuscript received 10 February 1992, in final form 3 February 1994)

ABSTRACT

The numerical study presented here focuses on baroclinic processes that contribute to tropical cyclone (TC) propagation. A three-dimensional, semispectral, primitive equation model of baroclinic vortex was developed to study TC motion.

In a tilted vortex, interaction between upper- and lower-level vorticity anomalies leads to vortex propagation relative to the steering flow. On a β plane, with no environmental flow, the vortex is tilted toward the south and the interaction between the layers reduces the westward movement of the vortex. The vortex tilting can also occur due to the vertical shear in the environmental wind. On an f plane, the interaction between the layers causes the northward movement of the vortex in westerly linear shear, and southward movement in easterly linear shear, with a meridional velocity of about 1 m s^{-1}. This velocity increases with increasing vortex intensity and vertical motion.

1. Introduction

The motion of tropical cyclones (TC) is usually described in terms of "steering" and "propagation." The "steering" describes the advection of the vortex by an environmental flow. The "propagation" corresponds to the processes involving an interaction between the vortex and environment.

In a highly simplified case of the barotropic nondivergent vortex moving in a uniform flow on an f plane, the conservation of vorticity implies that the vortex moves with the velocity of the flow—the motion is entirely due to "steering." The environment of observed tropical cyclones does not satisfy these conditions since the flow varies vertically and horizontally and interacts with the vortex. That makes it impossible to clearly distinguish between the vortex and the environmental flow, and as a consequence splitting the vortex motion into steering and propagation components is arbitrary. Nevertheless, the motion of a tropical cyclone can to a large extent be explained as advection by a large-scale flow (Chan and Gray 1982; Dong and Neumann 1986; Franklin 1990). The steering current is usually defined as vertical and azimuthal average of the flow in the vicinity of a tropical cyclone. The standard way to obtain the steering flow is to use the average wind for a radius 500–700 km and the layer 300–800 mb. However, different choices are possible, so the definition of the steering flow is not unique. In the numerical model in which the environmental flow is prescribed a priori, the partition of the flow for environmental and vortex component is simpler than in observations. In this paper the authors define the steering as due solely to the advection by the prescribed, initial, zonal flow.

Unlike "steering," the "propagation" depends also on vortex, and not only environmental, characteristics. Identifying the processes that influence cyclone propagation is an important aspect of tropical cyclone motion studies in which observational data and the results of analytical and numerical models play an equally significant role. Observations provide information on the typical values of cyclone propagation depending on synoptic situation, speed and direction of motion, and properties of the cyclone circulation (Chan and Gray 1982; Dong and Neumann 1986; Chan 1985; Gray 1991; Holland 1983; Holland 1984). An understanding

Corresponding author address: Dr. Maria Flatau, Scripps Institution of Oceanography, University of California at San Diego, La Jolla, CA 92093.

of the role different processes play in cyclone motion can be gained from analytical and numerical models. The barotropic processes governing the motion of tropical cyclones are fairly well known. Numerous studies have examined the role of planetary vorticity advection (Adem 1956; Holland 1983; Fiorino and Elsberry 1989b), environmental wind shear or vorticity gradients (Smith 1991; DeMaria 1987; Evans et al. 1991; Smith et al. 1990; Ulrich and Smith 1991), or vortex properties such as strength (especially the magnitude of the outer winds), size, and total angular momentum (Willoughby 1988; Shapiro and Ooyama 1990; Fiorino and Elsberry 1989a).

The influence of the vertical structure of a cyclone and its environment on cyclone motion has received less attention. Earlier, three-dimensional models (Kitade 1980; Madala and Piacsek 1975) supported the results of barotropic models and concluded that baroclinic vortices on the β plane move toward the northwest. Other three-dimensional models examined the role of vortex asymmetries in the absence of environmental effects (Anthes 1972; Abe 1987). Only recently has interest in the influence of baroclinic processes on cyclone motion begun to grow. Shapiro (1992) pointed out the impact of potential vorticity (not just absolute vorticity) on cyclone propagation. He has shown that even in the absence of absolute vorticity gradients, cyclones can propagate in the direction perpendicular to the zonal steering current. The propagation results from the fact that the temperature gradient associated with vertical shear causes the potential vorticity to change in the meridional direction.

Wang and Li (1992) investigated the role of vertical structure of the vortex in vortex motion on the β plane and concluded that a cyclonic vortex moves with speed proportional to its vertically averaged relative angular momentum.

On the other hand, Gray (1991) emphasized the role of baroclinic properties of the cyclone environment. He suggested that most tropical cyclone movement faster than the 5°–7° steering current results not from cyclone–environment interaction but from properties of the environment itself. Gray argued that the tilt of the trough in which the moving cyclone is embedded causes the vertically averaged wind to have a maximum near the cyclone center. When the standard 5°–7° wind averages are used, the maximum of the vertically averaged steering current is missed.

Another baroclinic mechanism influencing the motion of tropical cyclones was indicated by Flatau (1991) and Wu and Emanuel (1993). They pointed out that even though in barotropic studies the cyclone can be represented by a cyclonic vortex, in reality an anticyclonic potential vorticity anomaly that surmounts the low-level cyclonic anomaly can influence the motion of the low-level vortex. When the centers of the low-level cyclone and upper-level anticyclone are displaced relative to each other, the vortices can interact in the manner similar to interaction of vortices on a horizontal plane (Gryanik and Tevs 1989). The circulation induced by the low-level potential vorticity (PV) maximum causes the counterclockwise motion of the anticyclone, while the circulation induced by upper-level PV minimum causes clockwise motion of the cyclone. In the westerly shear, the upper-level anticyclone is located to the east of the low-level cyclone, and consequently the cyclone–anticyclone pair moves toward the north. In the easterly shear, when the anticyclone is to the west of the cyclone, the pair should move toward the south. When the displacement of the upper-level anticyclone is caused by the planetary vorticity advection, the anticyclone is positioned to the south of the cyclone, and the westerly motion of the vortex should be influenced by the interaction.

The goal of the numerical study presented here is to further investigate the role of this mechanism in propagation of a baroclinic vortex. The three-dimensional, primitive equation model of a baroclinic vortex described in section 2 is used to examine the propagation of the vortex on an f plane and a β plane. We consider the tilting of the vortex caused by the β effect (section 3) and by the vertically sheared environmental flow (section 4). Section 5 contains discussion of our results.

2. Three-dimensional model of a moving vortex

a. Governing equations

The baroclinic vortex model uses the nonlinear primitive equations formulated with cylindrical coordinates in the horizontal and the σ coordinate in the vertical. The vertical coordinate σ is defined as $\sigma = p/p_s$, where p_s is the surface pressure. [The coordinate $\sigma = (p - p_T)/(p_s - p_T)$ can also be used in the model. In this paper $p_T = 0$.] In the coordinates (r, λ, σ), the governing equations have the following form.

Pressure tendency equation:

$$\frac{\partial}{\partial t}(p_s r) = -\int_0^1 \frac{\partial}{\partial r}(p_s r u)d\sigma - \int_0^1 \frac{\partial}{\partial \lambda}(p_s v)d\sigma \quad (1)$$

Vertical velocity equation:

$$p_s r\dot{\sigma} = -\left(\sigma \frac{\partial}{\partial t}(p_s r) + \int_0^\sigma \frac{\partial}{\partial r}(p_s r u)d\sigma + \int_0^\sigma \frac{\partial}{\partial \lambda}(p_s v)d\sigma\right) \quad (2)$$

Hydrostatic equation:

$$\frac{\partial \Phi}{\partial \sigma} = -\frac{RT}{\sigma} \quad (3)$$

Radial momentum equation:

$$\frac{\partial}{\partial t}(p_s r u) = -\frac{\partial}{\partial r}(p_s r u u) - \frac{\partial}{\partial \lambda}(p_s v u) - \frac{\partial}{\partial \sigma}(p_s r u \dot{\sigma}) + \left(f + \frac{v}{r}\right) p_s r v - p_s r \frac{\partial \Phi}{\partial r} - rRT\frac{\partial p_s}{\partial r} \quad (4)$$

Tangential momentum equation:

$$\frac{\partial}{\partial t}(p_s r v) = -\frac{\partial}{\partial r}(p_s r u v) - \frac{\partial}{\partial \lambda}(p_s v v) - \frac{\partial}{\partial \sigma}(p_s v r \dot{\sigma}) - \left(f + \frac{v}{r}\right) p_s r u - p_s \frac{\partial \Phi}{\partial \lambda} - RT\frac{\partial p_s}{\partial \lambda} \quad (5)$$

Potential temperature equation:

$$\frac{\partial}{\partial t}(p_s r \theta) = -\frac{\partial}{\partial r}(p_s r u \theta) - \frac{\partial}{\partial \lambda}(p_s v \theta) - \frac{\partial}{\partial \sigma}(p_s r \dot{\sigma} \theta) + r p_s Q, \quad (6)$$

where u and v are radial and tangential velocities, $\dot{\sigma}$ is the vertical velocity in σ coordinates, θ and T are potential temperature and temperature, ϕ is geopotential, R is the gas constant, and Q denotes a diabatic heat source.

The model equations do not include moist processes explicitly and the diabatic heat source is specified. We assume that the heat source is symmetric with respect to the vortex center. Following Hack and Schubert (1986), the heating function approximates the apparent heat source from Yanai et al. (1973) and has the form

$$Q = a\hat{Q}\sin(\pi\sigma)\exp(-\alpha\sigma)\exp(-r^2/r_0^2), \quad (7)$$

where $\hat{Q} = 7.87$°C/day, $\alpha = 0.554$, $r_0 = 150$ km, and a is a normalization factor assuring that the horizontally averaged heating within the certain radius r_1 (in our calculation $r_1 = 250$ km) is equal to $Q(z)$, where $Q(z)$ is a heating profile from Yanai et al. (1973). We assume that the magnitude of the heat source does not change with time and that the distribution is constant relative to the vortex center. A more detailed description of the numerical model can be found in Flatau and Stevens (1993). Here we highlight only the most important features of the model.

The model consists of five equally spaced layers. In the lowest layer, small Newtonian friction (with e-folding timescale of 5 days) is included to partially compensate the energy from diabatic heating, but since we focus our investigation on the interaction with upper layers of the vortex, we do not include in the model the boundary-layer physics. As shown by Kuo (1969), including the frictional effects leads to the rightward deflection of the vortex from its path determined by the steering flow.

The model is half-spectral in the horizontal with Fourier representation in the azimuthal direction and finite differencing in radial direction. All the model variables are expressed as

$$X(r, \lambda, \sigma) = \sum_{s=-S}^{S} x_s(r, \sigma)\exp(is\lambda). \quad (8)$$

Because all the X variables are real, the coefficients x_{-s} are complex conjugates of x_s, and for every σ and r we need to solve $S + 1$ equations. Such a representation allows a limitation of the number of tangential modes necessary to describe three-dimensional features of the moving vortex. In some barotropic linear models of the moving vortex (Willoughby 1988; Peng and Williams 1990), the asymmetries are limited to tangential wavenumber $s = 1$. Since the motion of the vortex is determined by the flow near the vortex center and $s = 1$ is the only spectral component with nonvanishing amplitude at $r = 0$, most of the information on the vortex motion is contained in this wavenumber. However, in a nonlinear model the wave–wave interaction can also contribute to the $s = 1$ mode. As we have shown earlier (Flatau and Stevens 1989), the asymmetries with wavenumbers 1 and 2 can develop spontaneously in an outflow layer of the tropical cyclone. Therefore, we decided to include also wavenumbers 2 and 3 in our calculations, even though the environmental flow used in our experiments has only $s = 1$ component. The effect of including more than three azimuthal modes on the track of an initially symmetric vortex (Fig. 1),

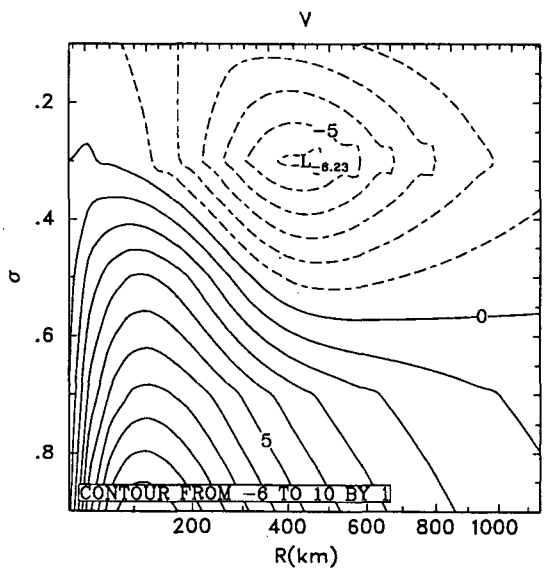

FIG. 1. Tangential velocity in the initial symmetric vortex.

moving in the zonally uniform flow with easterly shear, is shown in Fig. 2. Even though the vortices do not follow exactly the same track, their directions and speeds are similar in all the cases, with the vortex with five azimuthal components moving slightly slower. Since in this paper we concentrate on general characteristics of the motion of a baroclinic vortex, the spectral decomposition was truncated on third azimuthal wavenumber.

The model is formulated in the coordinate system stationary with respect to earth. Such formulation creates two problems. One is similar to that encountered in nested grids models—the center of the vortex "escapes" from the area where the coordinate stretching and Fourier expansion provide the finest resolution. Another problem results from the use of the spectral representation of the variables. When the vortex center is too far from the coordinate center, the asymmetries are mainly the result of this mismatch and not the vortex dynamics. This is an especially undesirable feature in the case of the pressure field. Since we use a Taylor expansion to calculate some of the nonlinear terms involving the surface pressure, it is quite important that the surface pressure be as symmetric as possible.

To deal with these problems, we use a procedure similar to that in Jones (1977) and Kurihara and Bender (1980) and relocate the coordinate center to match the vortex center if the distance between them exceeds the prescribed limit r_d.

The definition of the vortex center is based on the surface pressure field. In observations, the surface pressure contours near to the cyclone center rather closely approximate a circle. We define the vortex center as the center of such a circle. To calculate it we choose the pressure contour and fit the circle to this contour using the least squares method. That way, the asymmetric component of the pressure field is minimized. Choosing different pressure contours gives similar results, but care must be taken to choose a closed contour. The vortex center is calculated every hour using the pressure contour at a radius ~40 km. Since the heating function is defined relative to the vortex center and not the coordinate center, the heating distribution has to be calculated to correspond to the new vortex center.

After the distance between the vortex center and coordinate center exceeds r_d, the coordinate system is relocated and all variables are interpolated in the new coordinates. The magnitude of r_d is chosen depending on intensity of the vortex. For large, weak vortices the gradients of variables near the vortex center are not very large, and asymmetries created by vortex displacement are small compared to the symmetric flow. As the vortex begins to intensify, the tangential wind maximum increases and moves toward the center, and the variables change rapidly at small radii. In this case, even small displacements of the vortex create large asymmetries and r_d has to be small. In our model we use r_d between 20 and 5 km depending on intensity of the vortex. The values of r_d were determined experimentally, by running the interpolation scheme back and forth and comparing the fields before and after interpolation.

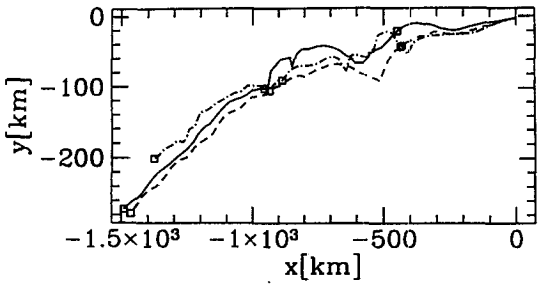

FIG. 2. Motion of the initially symmetric vortex in a zonally uniform flow with easterly shear. Solid line: truncation at azimuthal wavenumber $s = 3$, dashed line: truncation at $s = 4$, dot–dashed line: truncation at $s = 5$.

3. Movement of a baroclinic vortex on the β plane

The movement of a barotropic vortex on the β plane can be easily understood if we consider the vortex as a "packet" of Rossby waves with the outer circulation projected onto the longer waves and inner circulation projected onto the shorter waves (Chan and Williams 1987). Since Rossby waves move west due to the advection of the earth's vorticity, the vortex also moves west. However, longer waves move faster, creating a distortion of an initially symmetric vortex and thus asymmetric flow at the vortex center. The direction of this flow depends on whether the vortex is cyclonic or anticyclonic. In the cyclonic case, dispersion of Rossby waves causes northward flow at the center and northward movement of the vortex, while the anticyclonic vortex tends to move toward the south. This "linear" picture is modified by nonlinear interactions that hold the vortex together. This qualitative description of the movement of a vortex on the β plane is consistent with most of the results of nonlinear, barotropic models. All numerical models agree in their prediction of northwestward movement of cyclonic vortices. As indicated by analogy with Rossby waves, the speed of motion depends on size rather than intensity of the vortex (large vortices move faster). As shown by Fiorino and Elsberry (1989), changes of the larger (e.g., 1500 km) scales of the vortex circulation influence the vortex motion to a greater degree than smaller-scale (e.g., inner core) processes. The intensification of the vortex has a very small effect of the motion (Holland 1983; DeMaria 1987), even though according to classical work of Adem (1956) vortex intensity should determine its poleward speed.

Some features of a vortex moving on the β plane cannot be easily explained. The linear models (Willoughby 1988) suggest that the propagation of the vor-

tex is proportional to the total relative angular momentum (RAM) of the vortex. In Willoughby's linear, steady-state model, the vortex with zero angular momentum does not move. This simple relationship does not hold for the nonlinear calculations. Shapiro and Ooyama (1990) show that although the vortex with zero angular momentum is nondispersive to lowest order (and therefore our idealized picture would indicate no meridional motion), it still moves northwestward. They indicate that there is no simple way to tie the vortex motion to the total RAM of the vortex. Willoughby (1992) shows that in linear calculations the speed of the vortex on a β plane is influenced by barotropically unstable modes and the steady state observed in nonlinear calculations is not reached.

The situation becomes even more complicated in the case of a baroclinic vortex. Some investigators (Gray 1991; Wang and Li 1992) have suggested that the coupling between the lower cyclonic and upper anticyclonic layers, caused by secondary circulation, should reduce the β-induced vortex motion. In their study of motion of baroclinic vortices on the β plane, Wang and Li (1992) notice that for the purely cyclonic vortices the motion strongly depends on the vertically averaged RAM, even in the absence of diabatic heating. This relationship does not hold for the vortices consisting of a cyclone–anticyclone pair. In this case, motion of the vortex is entirely determined by the lower, cyclonic part of the vortex. Wang and Li argue that this difference is caused by the fact that unlike the case of purely cyclonic vortex, the vertical velocity induced by the presence of potential vorticity anomalies disappears at midlevels, causing the cyclone and anticyclone to move independently of each other. They speculate that the insertion of diabatic heating could cause the coupling between upper and lower layers and mutual cancellation of β drift. This hypothesis does not agree with the results of 3D hurricane models (Madala and Piacsek 1975; Kitade 1980; DeMaria 1983; Shapiro 1992) that indicate northwestward vortex movement on the β plane in the absence of environmental flow.

To test the sensitivity of β-induced vortex motion to the vertical coupling between the vortex layers, we run the model on the β plane with no environmental flow. All experiments in this section use the same initial vortex shown in Fig. 1. The initial vortex was obtained by integrating a symmetric version of the model for 4 days from the initial state with zero tangential wind and standard tropical (Jordan sounding) temperature profile.

Using the same initial conditions, we run three experiments. In the first experiment (βNI), there is no diabatic heating. Therefore, a secondary circulation driven by heating does not develop. In the second ($\beta D0$) experiment, symmetric diabatic heating is used. In addition to providing coupling between the layers, the introduction of the diabatic heating intensifies the symmetric vortex. Since strength of the vortex influences its motion on a β plane, we run a third experiment ($\beta D20$) in which we attempt to increase the vertical exchange of asymmetric momentum between the layers without changing the symmetric structure of a vortex. In experiment $\beta D20$ we introduce the additional mixing of momentum by vertical diffusion ($F_D = K\partial^2\mathbf{u}/\partial z^2$) with a constant diffusion coefficient $K = 20$ m^2 s^{-2}. The momentum mixing is included only in asymmetric components, in order to keep the symmetric structure of the vortex unchanged relative to that in experiment $\beta D0$. This assumption of mixing only asymmetric components is quite artificial, and it is used only in experiment ($\beta D20$) to illustrate the role of vertical momentum exchange.

The potential vorticity fields in experiments $\beta D0$ and βNI are shown in Figs. 3 and 4. The potential vorticity in coordinates (r, λ, σ) is calculated according to the formula:

$$P = \left\{\frac{1}{r}\left[\frac{\partial rv}{\partial r} - \frac{\partial u}{\partial \lambda} + \frac{\sigma}{RT}\left(\frac{\partial \phi}{\partial r}\frac{\partial rv}{\partial \sigma} - \frac{\partial \phi}{\partial \lambda}\frac{\partial u}{\partial \sigma}\right)\right] + f\right\}\left(-\frac{\partial \theta}{\partial \sigma}\frac{g}{p_s}\right) - \frac{g}{rp_s}\frac{\partial u}{\partial \sigma}\left(\frac{\partial \theta}{\partial \lambda} + \frac{\sigma}{RT}\frac{\partial \phi}{\partial \lambda}\frac{\partial \theta}{\partial \sigma}\right) + \frac{g}{p_s}\left(\frac{\partial \theta}{\partial r} + \frac{\sigma}{RT}\frac{\partial \phi}{\partial r}\frac{\partial \theta}{\partial \sigma}\right). \quad (9)$$

The potential vorticity fields in this paper are presented using the normalized potential vorticity $P_n = P/P_{nn}$, where normalization factor P_{nn} is given by

$$P_{nn} = -f_0\frac{\theta(\sigma_T) - \theta(\sigma_B)}{(\sigma_T - \sigma_B)}\frac{g}{p_0}. \quad (10)$$

The 800-mb potential vorticity fields (Fig. 3) display all of the "classical" characteristics of a vortex moving on the β plane. The earth's vorticity is advected by the vortex circulation, creating an increase of potential vorticity west of the vortex and a decrease of potential vorticity to the east. The resulting wind asymmetry advects the vortex toward the northwest. The potential vorticity fields for βNI and $\beta D0$ at this level are similar, although without diabatic heating the vortex in the βNI case is less intense.

At 200 mb, the potential vorticity fields are quite different (Fig. 4). In βNI the upper-level negative anomaly is displaced toward the south relative to the low-level vortex, due to the advection of the earth's vorticity by the anticyclonic circulation. In $\beta D0$ the

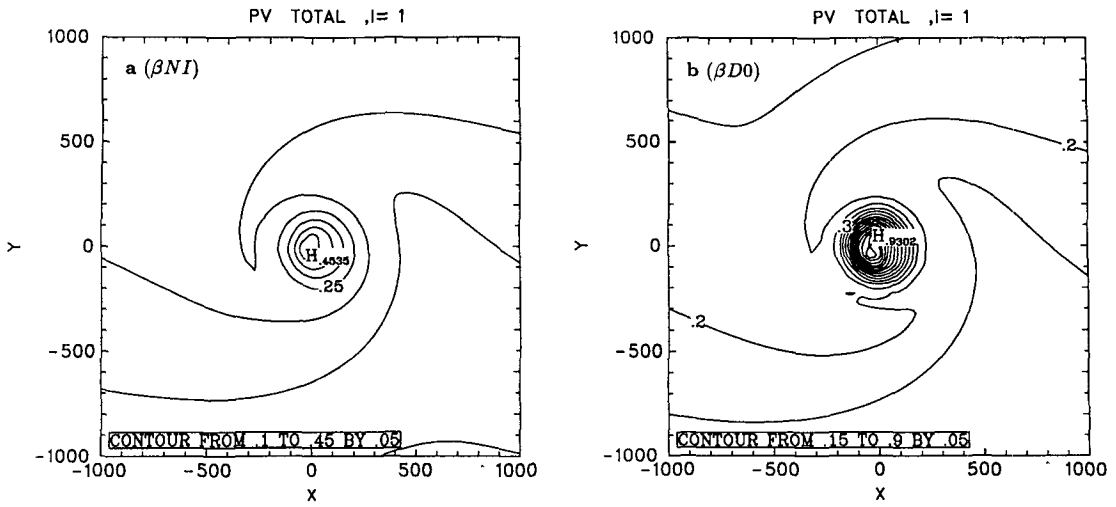

FIG. 3. Potential vorticity at 800 mb after 48 hours of integration. (a) Experiment βNI (no diabatic heating, no vertical diffusion), (b) experiment $\beta D0$ (diabatic heating, no diffusion). In this figure as well as in Figs. 4, 6, 7, and 11, the origin of the coordinate system coincides with the center of the low-level vortex.

200-mb potential vorticity pattern is much more complicated. The advective effects of the background vorticity by the vortex circulation can still be seen, but in addition the secondary circulation transports high potential vorticity air from below, creating a maximum at the vortex center. These features are similar to those observed in the upper-layer potential vorticity field from Shapiro's (1992) hurricane model, even though our model does not include a convective parameterization.

Vortex tracks for experiments βNI, $\beta D0$, and $\beta D20$ are shown in Fig. 5. The coupling caused by the secondary circulation does not reduce the meridional speed of the vortex. This behavior contrasts with that of the cyclonic-only vortex from Wang and Li (1992). Even though the average RAM of the vortex is small, the vortex still moves northwestward. In fact, vortices in $\beta D0$ and $\beta D20$ move toward the north slightly faster than the weaker vortex in βNI. Therefore, in spite of vertical coupling, the motion of the vortex is determined by the strength of low-level, cyclonic circulation rather than vertically averaged RAM. Our sensitivity experiments show that the presence of an upper-level cyclonic anomaly acts upon the low-level vortex in a manner described in the introduction, and circulation induced by the upper-level vortex reduces the westward velocity of the cyclone. Increasing the coupling by including momentum diffusion further diminishes the westward motion of the vortex.

Despite the small differences in westward propagation speed, vortices in all three experiments move toward the northwest. As in other nonlinear models, they initially move toward the north and then accelerate in the westward direction.

4. Baroclinic vortex in a vertically sheared flow

The tilt of the vortex considered in the previous section was caused by advection of environmental vorticity, and therefore we were not able to separate the influence of an upper PV anomaly from the β drift. In this section, we consider the case where the tilting of the vortex is caused by a vertically sheared environmental flow. First, we examine vortex motion on an f plane.

Even though the development of tropical cyclones is favored by minimum vertical shear, the tilting of the cyclones caused by vertically sheared flow has been observed (Huntley and Diercks 1981). This tilting usually occurs in the developing and dissipating stages. The tilt in the dissipating stage is often connected with westerly shear as the northward-moving cyclone encounters upper-level westerlies. This eastward tilt of the tropical cyclones moving in the westerly shear can be noticed in composite westward-moving cyclones, with the distance of about 500 km between low-level and upper-level circulation centers (Chan 1985).

To study the effect of vertical shear on vortex motion, we run three experiments. In the first, control experiment (CONT) the initial symmetric vortex moves in the uniform easterly ($u = -3$ m s^{-1}) current. In the next two experiments, we use the same initial vortex but an environmental flow has westerly (WF) and easterly (EF) shear.

The vertical shear in these experiments satisfies two conditions:

1) The vertical shear has to be relatively small. It is well known that large vertical shear inhibits development or even destroys the vortex. The "resistance" of

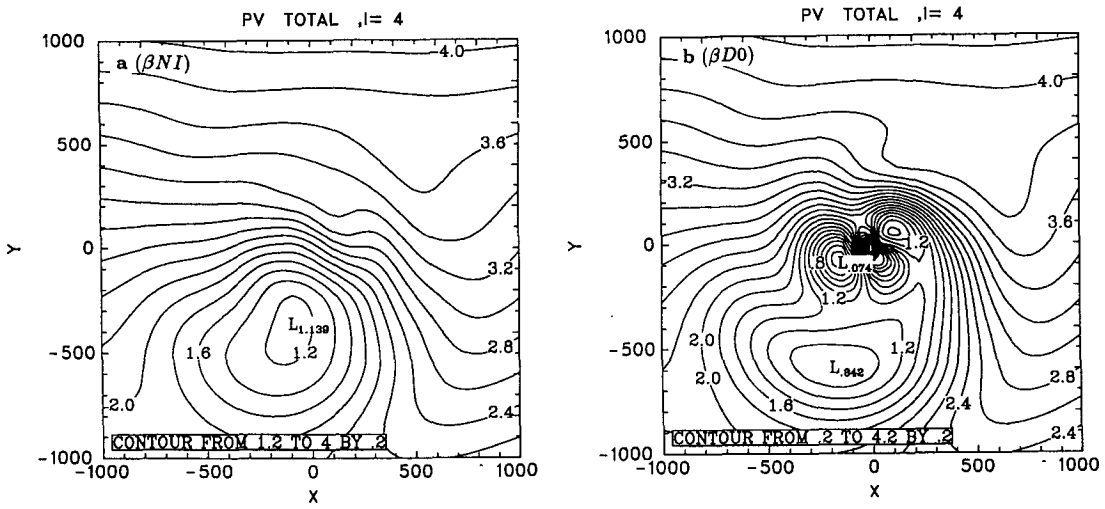

FIG. 4. Potential vorticity at 200 mb after 48 hours of integration. (a) Experiment βNI (no diabatic heating, no vertical diffusion) and (b) experiment $\beta D0$ (diabatic heating, no diffusion).

a hurricane to vertical shear depends on many factors. Observations show that hurricanes developing over warmer water can develop within more strongly sheared flow than those developing over a relatively cooler ocean. The phase speed of propagation of the upper-level disturbance relative to lower-level disturbance is also important (Tuleya and Kurihara 1981). However, tropical cyclones can usually withstand shears of 20 kt (9 m s^{-1}/600 mb) (M. DeMaria, personal communication).

2) The gradient of potential vorticity associated with the sheared flow has to be small. Even though there is no absolute vorticity gradient, the horizontal gradient of temperature resulting from thermal wind balance causes a difference in stability and therefore creates a gradient of potential vorticity. If this gradient is large, the effects observed in a numerical model result not from the interaction between upper and lower levels of the cyclone but from the advection of environmental vorticity, analogous to the β effect (Shapiro 1992).

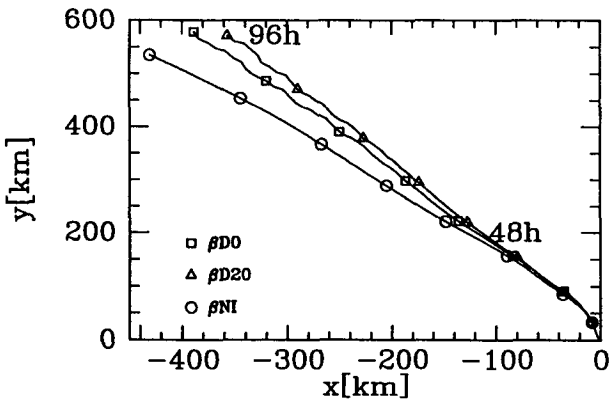

FIG. 5. Vortex tracks (β plane) in experiments βNI (no diabatic heating, no vertical diffusion), $\beta D0$ (diabatic heating, no diffusion), and $\beta D20$ (diabatic heating and vertical diffusion). The tracks are marked every 12 hours.

The initial flow used in the experiments consists of the sum of the vortex obtained from the symmetric version of the model (Fig. 1) and assumed zonal flow (called environmental flow in this section). The environmental flow is horizontally uniform and varies linearly with σ. The magnitude of the shear in experiments WF and EF is the same and equals 1.6 m s^{-1}/200 mb. The wind at the lowest level is -1.5 m s^{-1} for the easterly shear (EF) case and -3 m s^{-1} for the westerly shear (WF) case. The magnitude of the potential vorticity gradient in the environmental flow in experiments WF and EF is an order of magnitude smaller than that associated with the earth's vorticity gradient. The initial meridional potential vorticity gradient for the westerly shear case is 0.51 $\times 10^{-6}$ km^{-1} for potential vorticity calculated on the f plane and 0.72 $\times 10^{-5}$ km^{-1} if the calculation includes the planetary vorticity gradient.

The model was integrated for 3 days. When the vortex moves in a uniform flow, low- and upper-level vorticity extrema remain vertically aligned. For the westerly sheared flow (WF), the upper-level potential vorticity minimum after 24 h moves about 550 km to the east relative to the vortex center (Fig. 6). After 72 h (not shown) the potential vorticity minimum weakens and moves slightly farther toward the east. In addition, high potential vorticity air is advected from below, creating a potential vorticity maximum above the low-level vortex center. At the lower levels we can observe the advection of environmental potential vorticity by

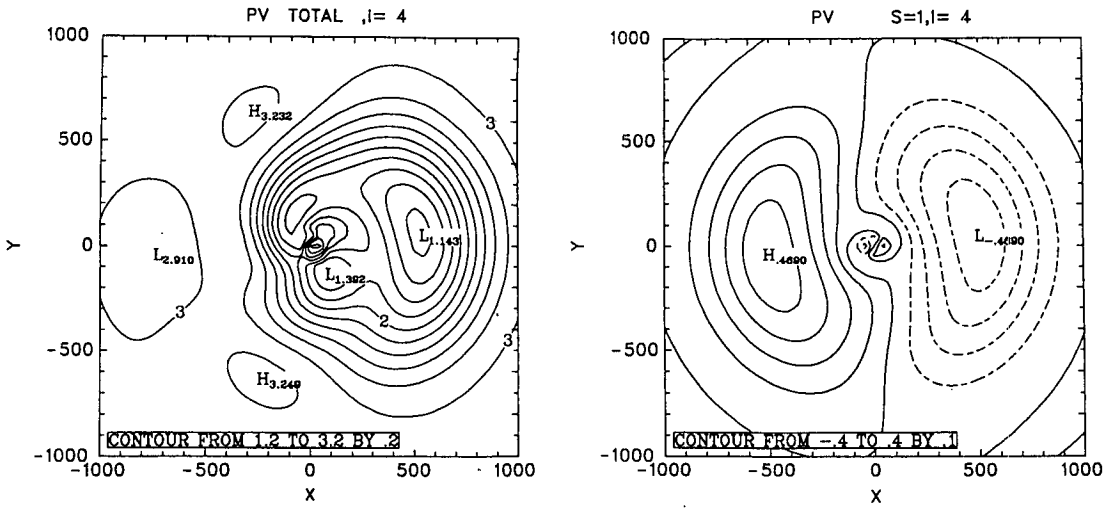

FIG. 6. Potential vorticity at 200 mb in experiment WF (westerly shear, f plane) after 24 hours of integration. (a) Total PV and (b) $s = 1$ component.

the vortex circulation. We should recall, however, that the gradient of environmental potential vorticity in this case is very small. In the easterly shear experiment (EF), the distribution of potential vorticity is similar except the upper-level minimum moves to the west relative to the low-level vortex.

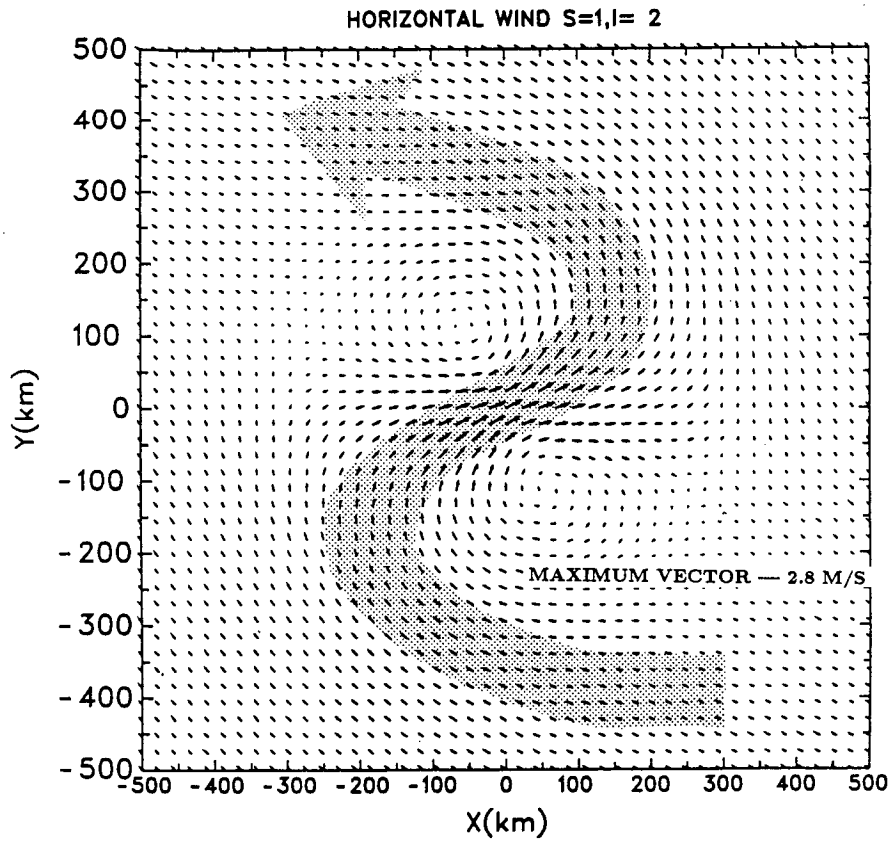

FIG. 7. Asymmetric flow ($s = 1$) at 700 mb in experiment WF (westerly shear, f plane) after 40 hours of integration.

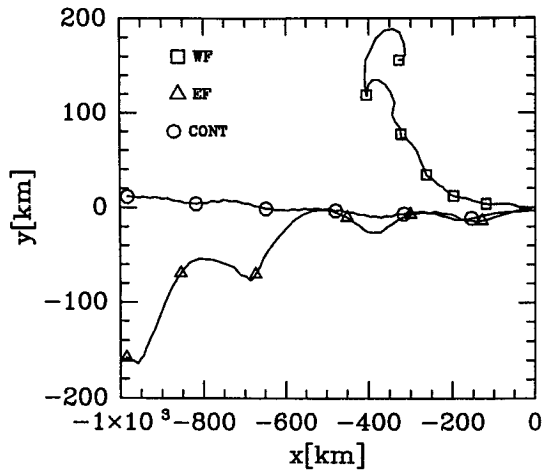

FIG. 8. Trajectory of the baroclinic vortices on the f plane in uniform easterly wind (CONT), westerly shear (WF), and easterly shear (EF) during 3 days of model integration. The tracks are marked every 12 hours.

Since, according to Gray (1991), the flow within a small radius (about 200 km) is the best indicator of vortex movement, we examine the $s = 1$ component of the flow near the vortex center. Even though initially the asymmetric flow was strictly in the east–west direction, after 40 h a meridional component of the flow is present at all levels (Fig. 7). In westerly shear (WF), the northward component of the flow averaged over the circle with radius 200 km increases with height from 0.12 m s^{-1} at 900 mb to 1.7 m s^{-1} at 300 mb. The vertical (900–300 mb) average is 0.8 m s^{-1}. For the easterly shear (EF), the flow near the vortex center acquires a southward component with a 900–300-mb average of 0.7 m s^{-1}.

Figure 8 shows the trajectories of the vortices in experiments CONT (uniform flow), WF (westerly shear), and EF (easterly shear) during 3 days of integration. In the vertically uniform flow the zonal velocity of the moving vortex is constant throughout the integration and is equal to the velocity of the environmental flow. The meridional velocity is almost zero except for a small deflection toward the north. This agrees with the theory of the motion of the vortex with friction (Kuo 1969) and the numerical results of Jones (1970, 1977) that predicts rightward deflection of the vortex path in the case of cyclonic vortex. Since our model does not include the boundary-layer effect but only a small Newtonian friction in the lowest layer, the meridional velocity induced by the frictional effects is small. When vertical shear is present, the vortices move initially with the low-level easterly flow. After about 24 h, we can see the effect of the vertical advection of zonal momentum by the secondary circulation; that is, the speed of the vortex becomes determined by the vertically averaged wind velocity rather than the low-level flow. The westward velocity of the vortex in easterly shear increases while the vortex moving in westerly shear slows down and eventually recurves. In the third day of calculation, the vortices move with speed close to the 900–300-mb average of the zonal environmental flow.

Since the initial environmental flow was strictly zonal with very small potential vorticity gradient, the meridional component of motion is caused by the interaction between the upper- and lower-level PV anomalies. As expected from our conceptual model, the vortex in westerly shear moves toward the north and the vortex in easterly shear moves toward the south. The speed of movement (about 1 m s^{-1} at 48 h) agrees quite well with the asymmetric component of the flow near the vortex center. The difference in meridional position between the vortex in easterly and westerly shear after 72 h of integration is about 350 km, and therefore has the magnitude comparable to that caused by the planetary vorticity advection by the same initial vortex in experiment $\beta D0$.

We now examine how the meridional motion of the vortex depends on the intensity of diabatic heating. We run additional experiments using the vortex in the westerly sheared flow. In experiment WF0 we turn off the diabatic heating after 24 h. As can be seen in Fig. 9, the meridional velocity in WF0 is smaller than that in experiment WF. The reduced coupling influences also the zonal velocity of the vortex. The vortex in WF0 moves faster toward the west, that is, with a velocity of the low-level flow. In an additional experiment (WF0A), we repeat WF0 but modify the vortex environment by decreasing the static stability. We expect that reduced stability should increase the vertical extent of the upper-level circulation and therefore amplify the interaction between the vortex levels. As recently

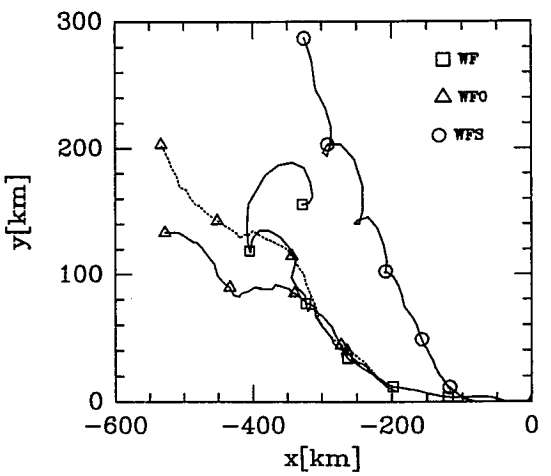

FIG. 9. Trajectories of the vortex in the westerly shear on an f plane. WF is the same as in the previous picture, WF0 denotes the experiment with no diabatic heating, WF0A (dashed line) is the same as WF0 except for the reduced static stability. In WFS the initial vortex velocity and intensity of diabatic heating is increased.

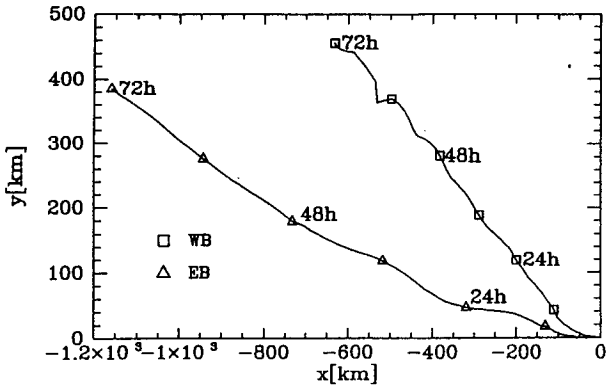

FIG. 10. Trajectory of the baroclinic vortices on the β plane, in experiments WB (westerly shear) and EB (easterly shear) during 3 days of model integration.

shown by Montgomery and Farrel (1992), an upper-level PV anomaly influences the vortex development to a much larger degree when the stability is reduced by including the moist processes in the atmosphere. In experiment WF0A, we decrease the stability by introducing the Rayleigh cooling of the upper troposphere (300 and 100 mb) by 1° relative to the initial temperature profile. Indeed, the vortex in experiment WF0A moves faster toward the north than that in WF0 (Fig. 9), although westward velocity stays the same.

In experiment WFS we increase the diabatic heating by a factor of 1.5. We also assume that the initial maximum wind in the symmetric vortex is 30 m s^{-1} instead of 10 m s^{-1}. Figure 9 indicates that the stronger vortex moves toward the north much more rapidly than the vortex in experiment WF.

In the next two experiments (WB, EB) we combine the effect of the vertical wind shear and β drift. We use zonal environmental flow with easterly and westerly shear so that earth's vorticity gradient is perpendicular to the flow. The trajectories of the vortices during 3 days of integration are shown in Fig. 10. Both vortices now move toward the north, with the vortex in westerly shear moving faster in the meridional direction than the one in easterly shear. However, the motion is not just a superposition of movements due to the β effect and the shear. The meridional difference between the positions of the vortices is now smaller than on the f plane (100 km instead of 350 km after 3 days). This effect can be explained by examining the corresponding potential vorticity fields (Fig. 11). The upper-level anticyclone not only is advected zonally by the sheared flow but also moves toward the south due to the advection of the planetary vorticity. Therefore, enhancement of the flow resulting from the interaction occurs in the southwestern sector of the upper-level vortex and southeastern part of the low-level vortex. The asymmetric flow caused by the interaction now induces the southwesterly instead of only the southerly component, and meridional motion decreases relatively to the case of shear flow on an f plane. This is in contrast to the situation described by Shapiro (1992), where the effects of shear-induced potential vorticity gradient and the β effect both contributed to the meridional potential vorticity gradient and therefore were additive. In the case of motion caused by interaction between upper- and lower-level PV anomalies, the direction of propagation depends on the position of these anomalies relative to each other, which is affected by the background potential vorticity gradient.

5. Summary and discussion

It is well known that vortices on a horizontal plane interact with each other; this interaction leads to prop-

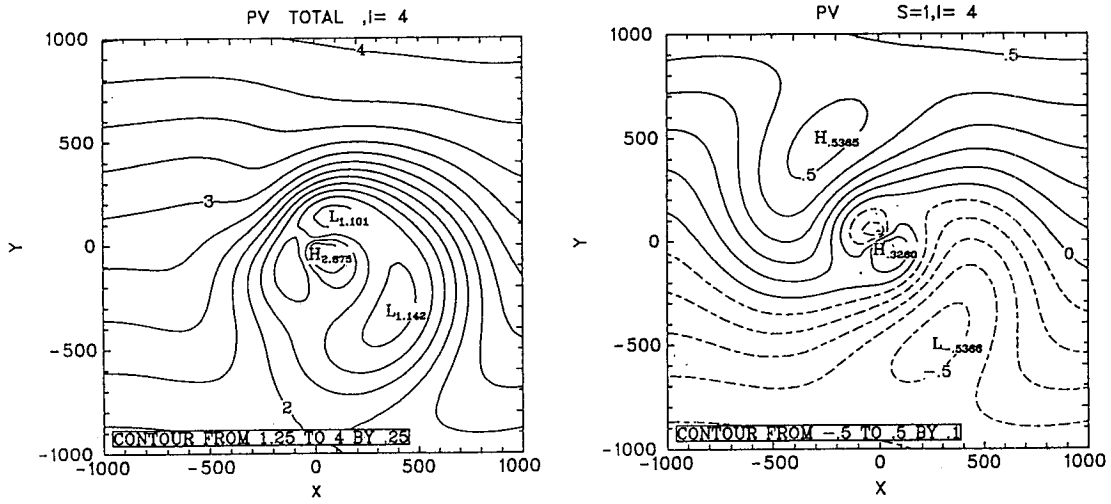

FIG. 11. Potential vorticity at 200 mb in experiment WB (westerly shear, β plane) after 24 hours of integration. (a) Total PV and (b) $s = 1$ component.

agation of vortices relative to the environmental flow. We have extended this idea to a tilted baroclinic vortex. In such a vortex the circulation in balance with the low-level PV anomaly advects the upper-level negative PV anomaly and vice versa. We have shown that the secondary circulation induced by the presence of diabatic heating additionally couples the vortex layers by upward advection of high PV air at the center and downward advection of low PV air at larger radius.

We considered vortex tilting caused by the β effect and vertically sheared environmental flow. Table 1 contains the summary of the experiments and the meridional vortex velocity obtained in each of the experiments.

In the linearly sheared environmental flow on an f plane, propagation due to interaction between the vortex layers is comparable to motion caused by the β effect for the same vortex. The speed of propagation increases with increased vortex intensity and magnitude of diabatic heating. In westerly linear shear, the vortex moves toward the north, while in easterly shear the interaction between vortex layers leads to southward propagation. This is in contrast with the results of Shapiro (1992), who found southward propagation in westerly sheared environmental flow. This apparent contradiction may be explained by the fact that, while both Shapiro's model and our model include the propagation caused by vertical interaction between the layers and horizontal transport of potential vorticity, the relative contribution of these mechanisms depends strongly on the wind profile and not only on the direction of the shear.

Consider the meridional gradient of potential vorticity caused solely by the presence of vertical shear in the u component. We will use the vertical coordinate z (pseudoheight) defined as

$$z = \left[1 - \left(\frac{p}{p_0}\right)^{\kappa}\right] \frac{c_p \theta_0}{g}, \tag{11}$$

where $\kappa = R/c_p$. In coordinates (x, y, z) the thermal wind equation has a simple form:

$$-f \frac{\partial u_g}{\partial z} = \frac{g}{\theta_0} \frac{\partial \theta}{\partial y}. \tag{12}$$

If we assume that vertical wind shear is horizontally uniform and there is no absolute vorticity gradient, the meridional gradient of potential vorticity is determined by the second derivative of u_g:

$$\frac{\partial q}{\partial y} \sim f \frac{\partial}{\partial z}\left(\frac{\partial \theta}{\partial y}\right) \sim -\frac{\partial^2 u_g}{\partial z^2}. \tag{13}$$

If the wind change is linear in z, there is no potential vorticity gradient associated with stability changes, and the vortex propagation is caused solely by an interaction between upper and lower layers of a cyclone. In our calculation shown in section 4, the wind change is linear in σ, so we observe a small meridional gradient of potential vorticity. This gradient, however, is much smaller (an order of magnitude) than the potential vorticity gradient caused by changing f, and therefore the contribution of horizontal vorticity advection to vortex propagation is very small. If, as in the case described by Shapiro (1992), the westerly shear increases with height, stability and potential vorticity decreases toward the north and the environmental potential vorticity advection causes the vortex to move toward the south.

In Fig. 12, we show the track of the vortex in westerly shear concentrated in the upper layers (experiment WFI), similar to that used in Shapiro (1992). The environmental wind is equal to zero at lower levels and increases rapidly between 500 and 300 mb with the maximum of 8 m s^{-1} at 300 mb. In spite of the 900–200 mb difference in horizontal wind being the same as in the experiment WF, the vortex in Fig. 12 moves toward the south, that is, in the direction opposite to that observed in experiment WF. Therefore, careful analysis of the environmental wind profile and vortex structure is necessary to predict the direction and speed of propagation of a baroclinic vortex in sheared flow. The results of this experiment as well as experiments WB and EB indicate also that in spite of the significant effect of vertical interaction of upper- and lower-level

TABLE 1. List of experiments.

Experiment	β/f	Vertical coupling	Environmental flow	V_v (m s^{-1})
βNI	β	no heating	—	1.38
$\beta D0$	β	diabatic heating	—	1.50
$\beta D20$	β	diabatic heating + vertical diffusion	—	1.50
CONT	f	diabatic heating	uniform zonal flow 3 m s^{-1}	0.05
WF	f	diabatic heating	linear westerly shear	0.61
WF0	f	no heating	linear westerly shear	0.52
WF0A	f	no heating, lower stability	linear westerly shear	0.79
WFS	f	stronger diabatic heating	linear westerly shear	1.14
WFI	f	diabatic heating	westerly shear between 500 and 300 mb	−0.77
WB	β	diabatic heating	linear westerly shear	1.74
EF	f	diabatic heating	linear easterly shear	−0.61
EB	β	diabatic heating	linear easterly shear	1.44

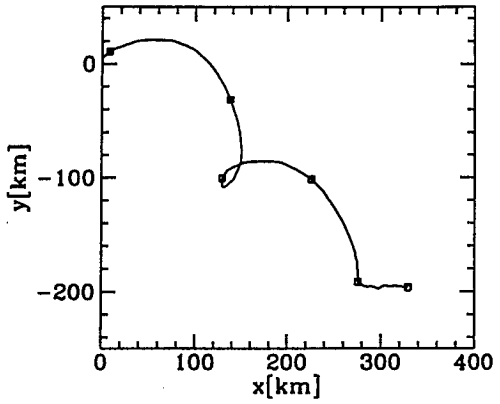

FIG. 12. The vortex track in the westerly shear concentrated in the layer 500–300 mb (WFI).

vortex in the absence of horizontal PV gradient, horizontal PV advection remains the primary mechanism of vortex propagation.

A similar conclusion is true for a vortex on the β plane in the absence of environmental flow. Even though the baroclinic effects modify the β drift, a baroclinic vortex on the β plane moves toward the northwest as predicted by barotropic models. The interaction between upper and lower layers of the vortex reduces the westward speed of a cyclone. Increasing the vertical exchange between layers by introducing vertical momentum advection by secondary circulation and momentum diffusion further reduces the westward velocity, without noticeable changes in the meridional velocity of the vortex. It is interesting to note that the introduction of an anticyclonic circulation on the periphery of a barotropic vortex reduces the poleward velocity of the vortex, while an introduction of an anticyclonic circulation at the top of a cyclone leads to a decrease in the westward velocity. This suggests that intuition gained from barotropic models cannot always be easily extended to baroclinic situations, and integrated qualities (for example, vertically integrated RAM) are not always good predictors of the vortex motion.

In this paper, we have neglected the effect of the horizontal distribution of diabatic heating. In all experiments described here, the diabatic heating is symmetric relative to the vortex center. In reality, the convection in a tropical cyclone is not necessarily symmetric. For example, introduction of a sheared flow causes an asymmetry in the vertical velocity and therefore asymmetry of convection. Different sea surface temperatures or the presence of moist, humid air on the equatorward side of the cyclone can also lead to the asymmetric heating. The effects of asymmetric distributions of diabatic heating on vortex motion will be investigated in the second part of this paper.

Acknowledgments. The authors are grateful to Dr. William Gray, Dr. Lloyd Shapiro, Paul Ciesielski, Dr. Roger Smith, and anonymous reviewers for their helpful comments and discussion. This work was sponsored by NSF under Grants ATM8352205, ATM8609731, and CCC00C4, and by the Office of Naval Research under Grant N000014-K-0214. Computing support was provided by the National Center for Atmospheric Research.

REFERENCES

Abe, S., 1987: The looping motion and the asymmetry of tropical cyclone. *J. Meteor. Soc. Japan,* **65,** 247–257.

Adem, J., 1956: A series solution for the barotropic vorticity equation and its application in the study of atmospheric vortices. *Tellus,* **8,** 364–372.

Anthes, R. A., 1972: Development of asymmetries in a three-dimensional numerical model of the tropical cyclone. *Mon. Wea. Rev.,* **100,** 461–476.

Chan, J. C. L., 1985: Identification of the steering flow for tropical cyclone motion from objectively analyzed fields. *Mon. Wea. Rev.,* **113,** 106–116.

——, and W. M. Gray, 1982: Tropical cyclone movement and surrounding flow relationships. *Mon. Wea. Rev.,* **11,** 1354–1374.

——, and R. T. Williams, 1987: Analytical and numerical studies of the beta-effect in tropical cyclone motion. Part I: Zero mean flow. *J. Atmos. Sci.,* **44,** 1257–1264.

DeMaria, M., 1983: Experiments with a spectral tropical cyclone model. Atmospheric Science Paper 371, 224 pp. [Available from Colorado State University, Fort Collins, CO 80523.]

——, 1987: Tropical cyclone motion in a nondivergent barotropic model. *Mon. Wea. Rev.,* **115,** 2346–2357.

Dong, K., and C. J. Neumann, 1986: The relationship between tropical cyclone motion and environmental geostrophic flows. *Mon. Wea. Rev.,* **114,** 115–122.

Evans, J. L., G. J. Holland, and R. L. Elsberry, 1991: Interactions between a barotropic vortex and an idealized subtropical ridge. Part I: Vortex motion. *J. Atmos. Sci.,* **48,** 301–314.

Fiorino, M., and R. L. Elsberry, 1989a: Contributions to tropical cyclone motion by small, medium and large scales in the initial vortex. *Mon. Wea. Rev.,* **117,** 721–727.

——, and ——, 1989b: Some aspects of vortex structure related to tropical cyclone motion. *J. Atmos. Sci.,* **46,** 975–990.

Flatau, M., 1991: The influence of baroclinic processes on tropical cyclone motion. *19th Conf. on Hurricanes and Tropical Meteorology,* Miami, FL, Amer. Meteor. Soc., 349–352.

——, and D. E. Stevens, 1989: Barotropic and inertial instabilities in a hurricane outflow layer. *Geophys. Astrophys. Fluid. Dyn.,* **47,** 1–18.

——, and ——, 1992: The influence of outflow layer instabilities on tropical cyclone motion. *J. Atmos. Sci.,* **50,** 1721–1733.

Franklin, J. L., 1990: Dropwindsonde observations of the environmental flow of hurricane Josephine (1984): Relationships to vortex motion. *Mon. Wea. Rev.,* **118,** 2732–2744.

Gray, W. M., 1991: Tropical cyclone propagation. *19th Conf. on Hurricanes and Tropical Meteorology,* Miami, FL, Amer. Meteor. Soc., 385–390.

Gryanik, V. M., and M. V. Tevs, 1989: Dynamics of singular vorticies in a *N*-layer model of the atmosphere. *Bull. USSR Acad. Sci. Atmos. Oceanic Phys.,* **25,** 179–188.

Hack, J. J., and W. H. Schubert, 1986: Nonlinear response of atmospheric vortices to heating by organized cumulus convection. *J. Atmos. Sci.,* **43,** 1559–1573.

Holland, G. J., 1983: Tropical cyclone motion: Environmental interaction plus a beta effect. *J. Atmos. Sci.,* **40,** 328–342.

——, 1984: Tropical cyclone motion: A comparison of theory and observation. *J. Atmos. Sci.,* **41,** 68–75.

Huntley, J. E., and J. W. Diercks, 1981: The occurrence of vertical tilt in tropical cyclones. *Mon. Wea. Rev.,* **109,** 1689–1700.

Jones, R. W., 1977: Vortex motion in a tropical cyclone model. *J. Atmos. Sci.,* **34,** 1528–1553.

Kitade, T., 1980: Numerical experiments of tropical cyclones on a plane with variable Coriolis parameter. *J. Meteor. Soc. Japan,* **58,** 471–488.

Kuo, H. L., 1969: Motions of vortices and circulating cylinder in shear flow with friction. *J. Atmos. Sci.,* **26,** 390–398.

Kurihara, Y., and M. A. Bender, 1980: Use of movable nested mesh model for tracking a small vortex. *Mon. Wea. Rev.,* **108,** 1792–1809.

Madala, R. V., and S. A. Piacsek, 1975: Numerical simulation of asymmetric hurricanes on a β-plane with vertical shear. *Tellus,* **27,** 453–467.

Montgomery, M. T., and B. Farrel, 1992: Tropical cyclone formation. *J. Atmos. Sci.,* **50,** 285–310.

Peng, M. S., and R. T. Williams, 1990: Dynamics of vortex asymmetries and their influence on a vortex motion on a β plane. *J. Atmos. Sci.,* **47,** 1987–2003.

Shapiro, L. J., 1992: Hurricane vortex motion and evolution in a three-layer model. *J. Atmos. Sci.,* **49,** 140–153.

——, and K. V. Ooyama, 1990: Barotropic vortex evolution on a beta plane. *J. Atmos. Sci.,* **47,** 170–187.

Smith, R., 1991: An analytic theory of tropical cyclone motion in a barotropic shear flow. *Quart. J. Roy. Meteor. Soc.,* **117,** 685–714.

Smith, R. K., W. Ulrich, and G. Dietachmayer, 1990: A numerical study of tropical cyclones using a barotropic model. Part I: The role of vortex asymmetries. *Quart. J. Roy. Meteor. Soc.,* **116,** 337–362.

Tuleya, R. E., and Y. Kurihara, 1981: A numerical study on the effects of environmental flow on tropical storm genesis. *Mon. Wea. Rev.,* **109,** 2487–2505.

Ulrich, W., and R. K. Smith, 1991: A numerical study of tropical cyclone motion using a barotropic model. II: Motion in spatially-varying large-scale flows. *Quart. J. Roy. Meteor. Soc.,* **117,** 107–124.

Wang, B., and X. Li, 1992: The beta drift of three-dimensional vortices: A numerical study. *Mon. Wea. Rev.,* **120,** 579–593.

Willoughby, H. E., 1988: Linear motion of a shallow-water, barotropic vortex. *J. Atmos. Sci.,* **45,** 1906–1928.

——, 1992: Linear motion of a shallow water barotropic vortex as an initial-value problem. *J. Atmos. Sci.,* **49,** 2015–2031.

Wu, C.-C., and K. A. Emanuel, 1993: Interaction of baroclinic vortex with background shear: Application to hurricane movement. *J. Atmos. Sci.,* **50,** 62–76.

Yanai, M., S. Esbensen, and J.-H. Chu, 1973: Determination of bulk properties of tropical cloud clusters from large-scale heat and moisture budgets. *J. Atmos. Sci.,* **30,** 611–627.